

# Analysis of the critical behavior associated with the antiferromagnetic transitions of $\text{LaMnO}_3$ and $\text{CaMnO}_3$

J. A. Souza,<sup>1,2,\*</sup> J. J. Neumeier,<sup>1</sup> B. D. White,<sup>1</sup> and Yi-Kou Yu<sup>3</sup>

<sup>1</sup>*Department of Physics, Montana State University, P.O. Box 173840, Bozeman, Montana 59717-3840, USA*

<sup>2</sup>*Centro de Ciências Naturais e Humanas, Universidade Federal do ABC, CEP 09090-400 Santo André, SP, Brazil*

<sup>3</sup>*National Center for Biotechnology Information, 8600 Rockville Pike, Bethesda, Maryland 20894, USA*

(Received 18 September 2009; revised manuscript received 31 March 2010; published 27 May 2010)

We apply a method for analyzing phase transitions to the well-known antiferromagnets  $\text{LaMnO}_3$  and  $\text{CaMnO}_3$  using high-resolution thermal-expansion data. The critical exponents associated with the specific heat ( $\alpha$ ) are obtained. Within experimental error, the results suggest that  $\text{LaMnO}_3$  and  $\text{CaMnO}_3$  belong to the same universality class. An additional byproduct of our analysis is estimates for the pressure derivative of the magnetic phase transition temperature.

DOI: [10.1103/PhysRevB.81.172410](https://doi.org/10.1103/PhysRevB.81.172410)

PACS number(s): 75.47.Lx

## I. INTRODUCTION

For the majority of systems, a thermodynamic phase transition results in a change in the order parameter (OP).<sup>1,3</sup> Cooperative interaction between magnetic spins, in the special case of a magnetic transition, leads to long-range ordering of the spins and the OP is generally taken to be the magnetization in ferromagnets ( $M$ ), or the sublattice magnetization in the case of antiferromagnets. Its nonzero value in the ordered phase corresponds to symmetry breaking of the system. In a so-called continuous (i.e., second-order) phase transition, the OP rises continuously from zero at the critical temperature ( $T_c$ ), while for those discontinuous transitions (i.e., first order), for which an OP can be defined, a jump is observed.<sup>1</sup> In both cases, an anomaly appears in basic thermodynamic quantities at  $T_c$ . Continuous phase transitions are characterized by the buildup of fluctuations in the OP near  $T_c$  and the subsequent divergence of them at  $T_c$ . The fluctuations correspond to short-range clusters of the ordered phase, which are not correlated with regard to their mutual position. The behavior of the system near  $T_c$  is described by divergences in the correlation length ( $\xi$ ), which in turn leads to divergences in physically measurable quantities such as the magnetic susceptibility. The molar heat capacity at constant pressure ( $C_p$ ) either diverges or experiences a jump or exhibits a cusp at  $T_c$ . In contrast, at a discontinuous phase transition  $\xi$  remains finite and  $C_p$  exhibits a spike<sup>2</sup> at  $T_c$ .

For continuous phase transitions, which are the subject of this work, the behavior of physical quantities such as spontaneous magnetization [ $M=M(H=0)$ ], magnetic susceptibility [ $\chi=(\partial M/\partial H)_{H\rightarrow 0}$ ],  $\xi$ , and  $C_p$  obey power laws of the reduced temperature,  $t\equiv(T-T_c)/T_c$ , governed by the critical exponents,  $\beta$ ,  $\gamma$ ,  $\nu$ , and  $\alpha$ , respectively, near  $T_c$ .<sup>1,3</sup> Herein, we are primarily interested in the critical exponent  $\alpha$ . The volume thermal-expansion coefficient times temperature ( $\Omega T$ ) and isothermal compressibility coefficient ( $\kappa$ ) scale with the same critical exponent<sup>4</sup> as  $C_p$ , ( $|t|^{-\alpha}$ ). The critical region is loosely defined by the reduced temperature range which is dominated by a power-law behavior characterized by a single critical exponent  $\alpha$ . Empirical observation has shown that for magnetic systems, the critical region begins around  $\log|t|\sim -1$ , which coincides approximately with the break down of molecular-field theory at about the same point.<sup>5</sup>

The critical exponents are universal in the sense that a wide range of materials exhibit the same exponents.<sup>1,3</sup> These universality classes depend on the spatial dimensionality of the system, its symmetry, the number of components which comprise the OP, and the range of the microscopic interaction responsible for the phase transition.<sup>1</sup>

In previous work,<sup>4</sup> we proposed a method for the simultaneous analysis of  $C_p$  and the volumetric thermal expansion coefficient  $\Omega$  at constant applied magnetic field  $B$ . This method reveals that  $C_p$  is an asymptotically linear function of  $\Omega T$  and for continuous phase transitions they scale according to

$$C_p = T \left( \frac{\partial S}{\partial T} \right)_c + v \Omega T \left( \frac{\partial P}{\partial T} \right)_c. \quad (1)$$

In this equation,  $S$  is the molar entropy,  $v$  is the molar volume, and the derivatives  $(\partial S/\partial T)_c$  and  $(\partial P/\partial T)_c$  are along the transition line. This relation holds for temperatures in the vicinity of  $T_c$  and reveals that in this region,  $C_p^*$  and  $\Omega T$  scale with the *same* critical exponent. In practice,  $C_p^*$  is defined as  $C_p^* \equiv C_p - [a + bT + T(\partial S/\partial T)_c]$ . The linear term reflects contributions from degrees of freedom decoupled from the lattice expansion associated with the phase transition. According to Eq. (1), a continuous phase transition must exhibit good overlap between  $C_p^*$  and  $\Omega T \lambda$ , where  $\lambda$  is a scale factor; note that  $v$  does not change significantly in the region where the overlap is physically significant. After subtraction of the linear term, Eq. (1) may be rewritten as<sup>4</sup>

$$\frac{dT_c}{dP} = \frac{v \Omega T}{C_p^*}. \quad (2)$$

Thus, this method can predict the pressure derivative  $dT_c/dP$ .

Near  $T_c$ ,  $C_p^*$  and  $\Omega T \lambda$  can be fitted by the expression

$$\Omega T \lambda \propto C_p^* = (A_{\pm}/\alpha_{\pm})|t|^{-\alpha_{\pm}} + B_{\pm} + Dt, \quad (3)$$

where  $(A_{\pm}/\alpha)|t|^{-\alpha}$  represents the leading contribution to the singularity of  $C_p$  and the linear term  $B_{\pm} + Dt$  represents a background contribution. The one-parameter scaling theory requires that  $\alpha_- = \alpha_+$  for continuous phase transition. If  $\alpha < 0$ ,  $C_p$  shows a cusplike transition, remains finite, and has

the value of  $B$  at  $T_c$ . In this case,  $B$  should be the same above and below  $T_c$ , [ $B_+ = B_-$ ]. On the other hand, if  $\alpha > 0$ ,  $C_p$  shows diverging behavior, becoming infinite at  $T_c$ . In that case, one should consider corrections to scaling due to non-linear scaling fields at  $t=0$ .<sup>6</sup> In essence, this arises because the second derivative of the free energy is not required, from a theoretical standpoint, to be continuous in the absence of the magnetic field. Therefore, the constant  $B$  may contain contributions associated with the phase transition (or decoupled from the regular background) and it may acquire different values<sup>6-8</sup> above and below  $T_c$ . When  $\alpha=0$ ,  $C_p$  can show a simple discontinuity or a logarithmic divergence at  $T_c$ , with no power-law dependence.<sup>1</sup>

We applied this method to magnetic transitions<sup>4,9,10</sup> on three occasions to determine  $\alpha$  using a high-resolution thermal-expansion technique.<sup>11</sup> In those cases,  $\alpha$  was found to be positive ( $\alpha > 0$ ). Here, we apply it to the antiferromagnets  $\text{LaMnO}_3$  and  $\text{CaMnO}_3$  revealing exponents  $\alpha = -0.13(3)$  and  $-0.12(2)$ , respectively.

$\text{LaMnO}_3$  and  $\text{CaMnO}_3$  samples were prepared using the conventional solid-state method. Heat capacity was measured using a Quantum Design physical properties measurement system employing a thermal relaxation technique.<sup>12</sup> High-resolution thermal-expansion measurements were performed using a fused quartz capacitive cell with a sensitivity<sup>11</sup> in  $\Delta l$  of  $0.1 \text{ \AA}$ . The relative sensitivity is at least 3 orders of magnitude better than that of diffraction methods. This resolution provides the high-quality data required for critical analysis. The average manganese valence was measured using iodometric titration. Under the assumption that La, Ca, and O have the valences of +3, +2, and -2, respectively, we found the oxygen content of  $\text{LaMnO}_3$  to be  $3.04 \pm 0.01$  and  $\text{CaMnO}_3$  to be  $3.00 \pm 0.01$ .

Heat capacity at constant pressure  $C_p$  and linear thermal-expansion coefficient  $\mu = [1/L(300 \text{ K})][d\Delta L/dT]$ , where  $L$  is the sample length (we have assumed that for our polycrystalline samples  $\Omega = 3\mu$ ), for  $\text{LaMnO}_3$  and  $\text{CaMnO}_3$ , are shown in Fig. 1. A distinct peak with  $\lambda$  shape in both  $C_p$  and  $\mu$  is observed at the paramagnetic to antiferromagnetic (AF) phase transition occurring at the Néel temperatures  $T_N = 135.5 \text{ K}$  and  $122.6 \text{ K}$  for  $\text{LaMnO}_3$  and  $\text{CaMnO}_3$ , respectively. A  $\lambda$ -shaped peak (or cusp) along with the absence of hysteresis<sup>13</sup> suggest a continuous phase transition. The rounding of the peak, most pronounced for  $\text{LaMnO}_3$  (see Fig. 1), can be associated with sample inhomogeneity. This effect is observed even in single crystals and is likely attributable to Mn, La, and/or oxygen defects.<sup>14,15</sup> Experimental contributions to the rounding of the peaks include the large measuring heat pulses in the relaxation technique.<sup>12</sup> Although this is absent in our thermal-expansion measurements, the temperature spacing between data points also contributes to rounding when we calculate  $\mu$  by numerical, point-by-point differentiation, from our sample length versus  $T$  data. However, we have found the thermal-expansion technique superior to  $C_p$  measurements in revealing this divergent behavior because it is less susceptible to finite-size effects.

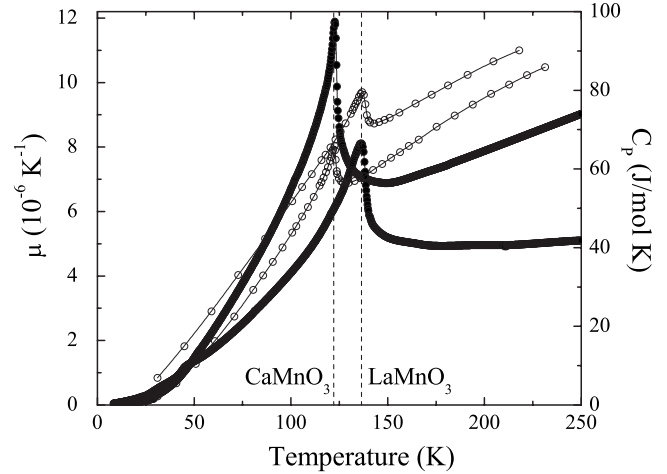


FIG. 1. Linear thermal-expansion coefficient  $\mu = \Omega/3$  (solid symbols) and heat capacity  $C_p$  (open symbols) for  $\text{CaMnO}_3$  and  $\text{LaMnO}_3$ . Dashed lines indicate phase transition temperatures.

To apply Eq. (1), we first subtract a linear contribution ( $a + b'T$ ) (where  $b' = [b + (\partial S/\partial T)_c]$ ) from  $C_p(T)$  (mimicking a conventional background) and find a rough value for the scale factor  $\lambda$  to collapse  $C_p^*$  and  $\mu T \lambda$  onto one curve. Afterwards, the constant  $a$ , linear coefficient  $b'$ , and  $\lambda$  values are refined to enlarge the overlap range between  $C_p^*$  and  $\mu T \lambda$ . Figure 2 shows the resulting overlap between  $C_p^*$  and  $\mu T \lambda$  suggesting a continuous phase transition for  $\text{LaMnO}_3$  and  $\text{CaMnO}_3$ . The scale factors  $\lambda$  are found to be  $27\,000 \pm 300 \text{ J/mol K}$  and  $26\,000 \pm 300 \text{ J/mol K}$ , respectively. Using Eq. (2) ( $v = 3.57 \times 10^{-5} \text{ m}^3/\text{mol}$ ), values of  $dT_N/dP = 3.9(6) \text{ K/GPa}$  and  $4.1(6) \text{ K/GPa}$  are obtained for  $\text{CaMnO}_3$  and  $\text{LaMnO}_3$ , respectively. These pressure derivatives obtained using our scaling method are in agreement with those measured experimentally ( $3.4 \text{ K/GPa}$  and  $5.4 \text{ K/GPa}$  for  $\text{CaMnO}_3$  and  $\text{LaMnO}_3$ , respectively).<sup>16</sup>

The critical exponent for each sample is obtained using the thermal-expansion data which have higher density of points and exhibit less rounding of the transition than the heat-capacity data. This difference is likely associated with finite-size effects.<sup>4,12,17,18</sup> Although more complicated fitting may be employed, we allow only a background subtraction using  $(\mu T \lambda - B_{\pm} - Dt) = (A_{\pm}/\alpha)|t|^{-\alpha}$ . First, we assume that  $\alpha > 0$  ( $C_p$  diverging transition) for  $\text{LaMnO}_3$  and  $\text{CaMnO}_3$  and choose  $B_{\pm}$ ,  $D$ , and  $T_c$  that maximize the power-law fitable temperature range of  $\mu T \lambda$  versus  $|t|$  on a  $\log_{10}$ - $\log_{10}$

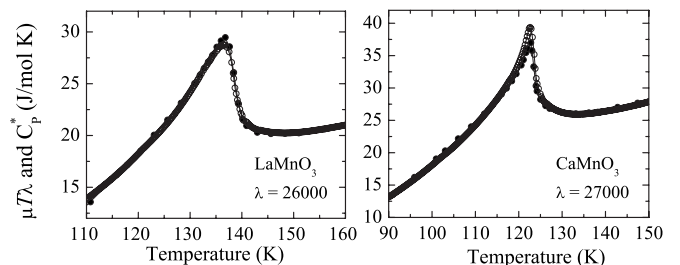


FIG. 2.  $C_p^*$  (solid symbols) and  $\mu T \lambda$  (open symbols) versus  $T$  illustrating the overlap between them.

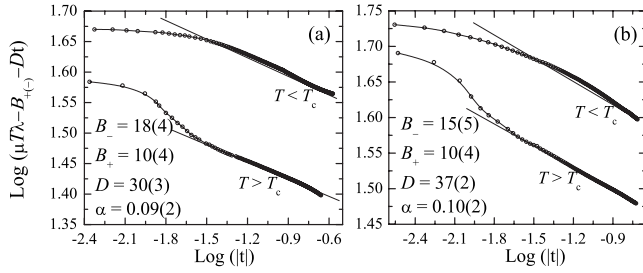


FIG. 3.  $\mu T \lambda - B_{\pm} - Dt$  as a function of the reduced temperature  $|t|$  on a  $\log_{10}$ - $\log_{10}$  scale above and below  $T_c$  for (a) LaMnO<sub>3</sub> and (b) CaMnO<sub>3</sub> assuming that  $\alpha$  is positive. Values of  $B$  and  $D$  are in J/mol K.

scale constraining  $\alpha_- = \alpha_+$ . Figures 3(a) and 3(b) display  $(\mu T \lambda - B_{\pm} - Dt)$  versus  $|t|$  on a  $\log_{10}$ - $\log_{10}$  scale above and below  $T_c$  for LaMnO<sub>3</sub> and CaMnO<sub>3</sub>, respectively. Careful inspection of Fig. 3 reveals poor linearity for  $T < T_c$  and a small linear temperature range. Since the above analysis with  $\alpha > 0$  is not so convincing, we let  $\alpha < 0$  implying  $(-\mu T \lambda + B_{\pm} + Dt) = (A_{\pm} / |\alpha|) |t|^{|\alpha|}$  and repeat the same procedure choosing  $B$ ,  $D$ , and  $T_c$  that maximize the linear temperature range. In this case,  $B$  is constrained to be the same above and below  $T_c$ . Figures 4(a) and 4(b) show the  $(-\mu T \lambda + B_{\pm} + Dt)$  versus  $|t|$  on a  $\log_{10}$ - $\log_{10}$  scale above and below  $T_c$  for LaMnO<sub>3</sub> and CaMnO<sub>3</sub>, respectively. The agreement of  $\alpha_+ = \alpha_-$  and the linear  $T$  range with one-parameter scaling theory is better. Notable is the improved linearity below  $T_c$  and a larger region of linearity (especially for  $T < T_c$  in the case of CaMnO<sub>3</sub>). The resulting parameters are,  $B_{\pm} = 45(4)$  J/mol K and  $D = 44(3)$  J/mol K for LaMnO<sub>3</sub> and  $B_{\pm} = 60(4)$  J/mol K and  $D = 50(3)$  J/mol K for CaMnO<sub>3</sub>. The critical exponent is determined as the slope of the linear region. Therefore, the inherent rounding of the transition close to  $T_c$  and the deviation from linearity are not included in determination of the slope. Though the reduced temperature range wherein our experimental data obey the critical behavior expression is small, it is inside of the  $|t| \leq -1$  boundary where the observation of true critical behavior is expected.<sup>5</sup> From the y intercept and the slope, we obtained the critical parameters:  $\alpha = -0.13(3)$  and  $A_+/A_- = 1.01(2)$  for LaMnO<sub>3</sub> and  $\alpha = -0.12(2)$  and  $A_+/A_- = 1.06(2)$  for CaMnO<sub>3</sub>. As discussed below, the values of  $\alpha$  and  $A_+/A_-$  suggest that both compounds are of the same universality class.

The negative values of  $\alpha$  imply that  $C_p^*$  is finite at  $T_c$  (i.e.,  $C_p^* = B$ ). The experimental values of  $C_p^*$  at  $T_c$  shown in Fig. 2 are 29.4 J/mol K and 39.4 J/mol K which have the same order of magnitude as those obtained through the scaling analysis 45(4) J/mol K and 60(4) J/mol K for LaMnO<sub>3</sub> and CaMnO<sub>3</sub>, respectively. We expect this agreement would be better if the inherent rounding were absent. The critical exponent for LaMnO<sub>3</sub> is in agreement with that obtained from thermal diffusivity [ $\alpha = -0.11(1)$ ] measurements.<sup>15</sup> This is the first time that  $\alpha$  is obtained for CaMnO<sub>3</sub>. At present, there are no analytical calculations of critical exponents for antiferromagnetic systems with which to compare our results but the three-dimensional ferromagnetic Heisenberg model

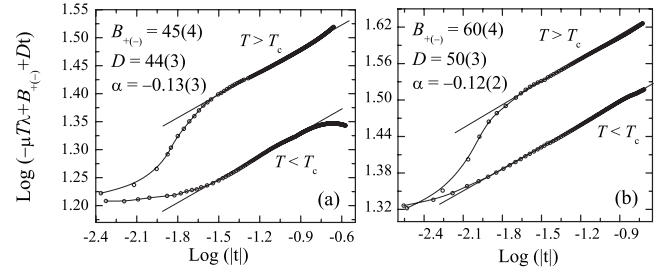


FIG. 4.  $-\mu T \lambda + B_{\pm} + Dt$  as a function of the reduced temperature  $|t|$  on a  $\log_{10}$ - $\log_{10}$  scale above and below  $T_c$  for (a) LaMnO<sub>3</sub> and (b) CaMnO<sub>3</sub> assuming that  $\alpha$  is negative. Values of  $B$  and  $D$  are in J/mol K.

was determined<sup>1</sup> to have  $\alpha = -0.11$  and  $A_+/A_- = 1.5$ . Numerous experimental determinations have been made including MnF<sub>2</sub> ( $\alpha = -0.103 \pm 0.03$ ),<sup>19</sup> Co<sub>3</sub>O<sub>4</sub> ( $\alpha = -0.15 \pm 0.06$ ),<sup>20</sup> RbMnF<sub>3</sub> ( $\alpha = -0.11 \pm 0.01$ ),<sup>21</sup> Sr<sub>2</sub>FeMoO<sub>6</sub> ( $\alpha = -0.12 \pm 0.01$ ),<sup>22</sup> CrO<sub>2</sub> ( $\alpha = -0.17$ ),<sup>23</sup> La<sub>0.9</sub>Ag<sub>0.1</sub>MnO<sub>3</sub> ( $\alpha = -0.127$ ),<sup>24</sup> NiO ( $\alpha = -0.118 \pm 0.006$ ),<sup>25</sup> and Ni ( $\alpha = -0.1 \pm 0.03$ ).<sup>26</sup> Comparing our results to these reveals that all values are negative and in the vicinity of  $-0.1$ .

CaMnO<sub>3</sub> orders with an isotropic G-type structure whereby each Mn magnetic moment is ordered antiferromagnetically with its nearest neighbor via superexchange interactions between Mn<sup>4+</sup> ions.<sup>27</sup> The ordering in LaMnO<sub>3</sub> is more complex because Mn<sup>3+</sup> has 4d electrons which leads to a Jahn-Teller effect and a tendency toward ferromagnetic order via the superexchange interaction.<sup>27-29</sup> It exhibits A-type AF order where the Mn magnetic moments in the  $a$ - $b$  plane are ferromagnetically ordered but successive planes are coupled antiferromagnetically. Thus, our findings reveal that despite the difference in the antiferromagnetic structures<sup>27,28</sup> exhibited by LaMnO<sub>3</sub> and CaMnO<sub>3</sub>, the critical exponents for both compounds, within experimental error, are identical as are the values of  $A_+/A_-$ . This indicates that LaMnO<sub>3</sub> and CaMnO<sub>3</sub> belong to the same universality class. On the other hand, another antiferromagnetic manganese oxide<sup>10</sup> CaMn<sub>2</sub>O<sub>4</sub> exhibits  $\alpha = 0.082 \pm 0.007$  suggesting a different universality class.

In summary, we have applied a method for analyzing continuous phase transitions to cusplike phase transitions ( $\alpha < 0$ ) where the heat capacity is finite at  $T_c$ . The critical exponents are determined for LaMnO<sub>3</sub> and CaMnO<sub>3</sub>. Within experimental error, both belong to the same universality class. This is somewhat surprising, given the differences in the antiferromagnetic ordered structures of the two compounds. Values for  $dT_c/dP$  were also determined.

This material is based upon work supported by the Brazilian agency CNPq (Grants No. 201017/2005-9, No. 471863/2008-4, and No. 307436/2008-0), National Science Foundation (Grant No. DMR-0504769), U.S. Department of Energy, Office of Basic Energy Sciences (Grant No. DE-FG-06ER46269) and the Intramural Research Program of the National Library of Medicine at the NIH.

\*joseantonio.souza@ufabc.edu.br

- <sup>1</sup>H. E. Stanley, *Introduction to Phase Transitions and Critical Phenomena* (Oxford University Press, New York, 1971).
- <sup>2</sup>F. Grønvdal, *J. Chem. Thermodyn.* **5**, 525 (1973).
- <sup>3</sup>M. E. Fisher, *Rep. Prog. Phys.* **30**, 615 (1967).
- <sup>4</sup>J. A. Souza, Yu. Yi-Kuo, J. J. Neumeier, H. Terashita, and R. F. Jardim, *Phys. Rev. Lett.* **94**, 207209 (2005).
- <sup>5</sup>L. P. Kadanoff, W. Götze, D. Hamblen, R. Hecht, E. A. S. Lewis, V. V. Paleiauskas, M. Rayl, J. Swift, D. Aspnes, and J. Kane, *Rev. Mod. Phys.* **39**, 395 (1967).
- <sup>6</sup>A. Aharony and M. E. Fisher, *Phys. Rev. B* **27**, 4394 (1983).
- <sup>7</sup>A. Kornblit and G. Ahlers, *Phys. Rev. B* **8**, 5163 (1973).
- <sup>8</sup>G. Ahlers and A. Kornblit, *Phys. Rev. B* **12**, 1938 (1975).
- <sup>9</sup>C. A. M. dos Santos, J. J. Neumeier, Yu. Yi-Kuo, R. K. Bollinger, R. Jin, D. Mandrus, and B. C. Sales, *Phys. Rev. B* **74**, 132402 (2006).
- <sup>10</sup>B. D. White, J. A. Souza, C. Chiorescu, J. J. Neumeier, and J. L. Cohn, *Phys. Rev. B* **79**, 104427 (2009).
- <sup>11</sup>J. J. Neumeier, T. Tomita, M. Debessai, J. S. Schilling, P. W. Barnes, D. G. Hinks, and J. D. Jorgensen, *Phys. Rev. B* **72**, 220505(R) (2005).
- <sup>12</sup>J. C. Lashley, M. F. Hundley, A. Migliori, J. L. Sarrao, P. G. Pagliuso, T. W. Darling, M. Jaime, J. C. Cooley, W. L. Hults, L. Morales, D. J. Thoma, J. L. Smith, J. Boerio-Goates, B. F. Woodfield, G. R. Stewart, R. A. Fisher, and N. E. Phillips, *Cryogenics* **43**, 369 (2003).
- <sup>13</sup>A. Szewczyk, M. Gutowska, and B. Dabrowski, *Phys. Rev. B* **72**, 224429 (2005).
- <sup>14</sup>J. A. M. Van Roosmalen, E. H. P. Cordfunke, and R. B. Helmholdt, *J. Solid State Chem.* **110**, 100 (1994).
- <sup>15</sup>A. Oleaga, A. Salazar, D. Prabhakaran, and A. T. Boothroyd, *J. Phys.: Condens. Matter* **17**, 6729 (2005).
- <sup>16</sup>J.-S. Zhou and J. B. Goodenough, *Phys. Rev. B* **68**, 054403 (2003).
- <sup>17</sup>J. A. Souza, J. J. Neumeier, and R. F. Jardim, *Phys. Rev. B* **75**, 012412 (2007).
- <sup>18</sup>J. J. Neumeier, M. F. Hundley, J. D. Thompson, and R. H. Heffner, *Phys. Rev. B* **52**, R7006 (1995).
- <sup>19</sup>I. Hatta and A. J. Ikushima, *Jpn. J. Appl. Phys., Part 1* **20**, 1995 (1981).
- <sup>20</sup>L. M. Khrilovich, E. V. Kholopov, and I. E. Paukov, *J. Chem. Thermodyn.* **14**, 207 (1982).
- <sup>21</sup>M. Marinelli, F. Mercuri, S. Foglietta, and D. P. Belanger, *Phys. Rev. B* **54**, 4087 (1996).
- <sup>22</sup>H. Yanagihara, W. Cheong, M. B. Salamon, S. Xu, and Y. Moritomo, *Phys. Rev. B* **65**, 092411 (2002).
- <sup>23</sup>H. Yanagihara and M. B. Salamon, *Phys. Rev. Lett.* **89**, 187201 (2002).
- <sup>24</sup>A. G. Gamzatov, S. B. Abdulvagidov, A. M. Aliev, K. S. Khizriev, A. B. Batdalov, O. V. Mel'nikov, O. Y. Gorbenco, and A. R. Kaul', *Phys. Solid State* **49**, 1769 (2007).
- <sup>25</sup>M. Massot, A. Oleaga, A. Salazar, D. Prabhakaran, M. Martin, P. Berthet, and G. Dhalenne, *Phys. Rev. B* **77**, 134438 (2008).
- <sup>26</sup>D. L. Connelly, J. S. Loomis, and D. E. Mapother, *Phys. Rev. B* **3**, 924 (1971).
- <sup>27</sup>P.-G. de Gennes, *Phys. Rev.* **118**, 141 (1960).
- <sup>28</sup>J. B. Goodenough, *Phys. Rev.* **171**, 466 (1968).
- <sup>29</sup>E. Dagotto, T. Hotta, and A. Moreo, *Phys. Rep.* **344**, 1 (2001).